Since January 2020 Elsevier has created a COVID-19 resource centre with free information in English and Mandarin on the novel coronavirus COVID-19. The COVID-19 resource centre is hosted on Elsevier Connect, the company's public news and information website.

American Journal of Infection Control 48 (2020) 1237–1243

Contents lists available at ScienceDirect

American Journal of Infection Control

journal homepage: www.ajicjournal.org

Major Article

Design and evaluation of a portable negative pressure hood with HEPA filtration to protect health care workers treating patients with transmissible respiratory infections

Hai-Thien Phu MD [1,a,b], Yensil Park PhD [1,c], Austin J. Andrews BS [c], Ian Marabella BS [c], Asish Abraham MD [d], Reid Mimmack BS [e], Bernard A. Olson PhD [c], Jonathan Chaika BS [f], Eugene Floersch BS [f], Mojca Remskar MD, PhD [d,f], Janet R. Hume MD, PhD [a], Gwenyth A. Fischer MD [a], Kumar Belani MD [d,*], Christopher J. Hogan Jr.PhD [c,**]

[a] University of Minnesota Medical School, Department of Pediatrics, Minneapolis, MN
[b] University of Minnesota Medical School, Division of General Internal Medicine, Minneapolis, MN
[c] University of Minnesota, Department of Mechanical Engineering, Minneapolis, MN
[d] University of Minnesota Medical School, Department of Anesthesiology, Minneapolis, MN
[e] University of Minnesota Medical School, Minneapolis, MN
[f] University of Minnesota, M Simulation, Minneapolis, MN

Keywords:
HEPA air filtration
Nosocomial infection
Aerosol based disease transmission

A B S T R A C T

Background: To mitigate potential exposure of healthcare workers (HCWs) to SARS-CoV-2 via aerosol routes, we have developed a portable hood which not only creates a barrier between HCW and patient, but also utilizes negative pressure with filtration of aerosols by a high-efficiency particulate air filter.

Material and Methods: The hood has iris-port openings for access to the patient, and an opening large enough for a patient's head and upper torso. The top of the hood is a high-efficiency particulate air filter connected to a blower to apply negative pressure. We determined the aerosol penetration from outside to inside in laboratory experiments.

Results: The penetration of particles from within the hood to the breathing zones of HCWs outside the hood was near 10^{-4} (0.01%) in the 200-400 nm size range, and near 10^{-3} (0.1%) for smaller particles. Penetration values for particles in the 500 nm-5 μm range were below 10^{-2} (1%). Fluorometric analysis of deposited fluorescein particles on the personal protective equipment of an HCW revealed that negative pressure reduces particle deposition both outside and inside the hood.

Conclusions: We find that negative pressure hoods can be effective controls to mitigate aerosol exposure to HCWs, while simultaneously allowing access to patients.

INTRODUCTION

The severe acute respiratory syndrome coronavirus (SARS-CoV-2 or COVID-19) pandemic, which spread globally beginning in early 2020, has been characterized by acute respiratory failure, suspected to be from multiple etiologies, such as acute respiratory distress syndrome from both direct and indirect lung injuries, pulmonary edema, and coagulation dysfunction resulting in microvascular thrombosis.[1] This has resulted in extreme stress on hospital systems due to the

* Address correspondence to Kumar Belani, MD, University of Minnesota Medical School, Department of Anesthesiology, Minneapolis, MN 55455 ** Address correspondence to Chris Hogan PhD, University of Minnesota, M Simulation, Minneapolis, MN 55455

E-mail addresses: belan001@umn.edu (K. Belani), hogan108@umn.edu (C.J. Hogan).

Funding: The authors acknowledge support from the University of Minnesota COVID-19 Rapid Response Grant Program and the Institute for Engineering in Medicine (IEM).

Conflicts of interest: None to report.

[1] Contributed equally to this project.

https://doi.org/10.1016/j.ajic.2020.06.203

need for prolonged ventilatory support for a large proportion of patients in a very acute period of time.

An accompanying issue is that personal protective equipment (PPE) and airborne isolation rooms are limited in availability, and there is concern of transmission to health care workers (HCWs) via droplet and aerosol routes. The CDC and WHO[2,3] have recommended against the use of many forms of noninvasive ventilation (NIV), such as BiPAP, CPAP, HFNC, with volumetric flow rates in excess of 6 L min^{-1}. There is evidence that respiratory droplets and smaller particles contain transmissible coronavirus,[4-6] and presently there is concern that NIV might increase aerosolization of patients' respiratory secretions.[7,8] In an effort to reduce nosocomial spread of coronavirus, an early intubation policy was also adopted for patients with respiratory failure, limiting most NIV systems for respiratory care.[2,3] Extubation of patients who in normal circumstances would be supported by NIV is also not recommended due to the risk of aerosolized spread of the virus and increased exposure to surrounding health care providers.

Ideally, patients with SARS-infection should be cared for in negative pressure rooms, and HCWs should don appropriate PPE to reduce their risk of infection.[2] The availability of airborne isolation rooms in the event of a pandemic was studied and methods to improve surge capacity were discussed after the SARS epidemic of 2003. Some of these solutions included transformation of wards into negative pressure wards specifically for infected patients.[9] This may not be achievable in all settings due to time and resource constraints. For this reason, we suggest that a portable negative pressure system to isolate patients in existing environments is an option to reduce the potential for aerosol transmission. Such a system would also provide additional protection for HCWs with limited PPE availability. To this end, we have designed and tested a portable *Aerosol Hood*, which builds upon the design of the *Aerosol Box*.[10] The *Aerosol Box*, conceived by Dr. Lai Hsien-Yung, is a rigid, partial enclosure that circumscribes a patient's head and upper torso, enabling provider access to the patient while also acting as a surface around the patient for the inertial impaction of larger respiratory droplets. However, while protection is provided against large (supermicrometer) inertial droplets and particles, in the *Aerosol Box* there is little-to-no protection from smaller (micrometer-to-submicrometer) aerosol particles, which would then be dispersed throughout the room upon removal of the box. The *Aerosol Hood* provides the same level of provider access (with 2 additional side openings for multiple personnel), but, like the ventilated headboards developed by the National Institute of Occupational Health & Safety,[11] includes a negative pressure system and a high-efficiency particulate air (HEPA) filter. With the filter mounted on the top of the device, the prototype has a flow profile similar to a fume hood, as well as to residential and industrial kitchen ventilation hoods. The *Aerosol Hood* hence provides both the ability to collect large droplets via impaction and smaller aerosol particles via HEPA filtration. Room air is continuously entrained into the hood at rate exceeding the flow rate of all NIV procedures by multiple orders of magnitude. The net result is protection for providers during potentially aerosol-generating procedures, such as endotracheal intubation. The hood may also facilitate extubation to NIV by containing and filtering the aerosolized particles and droplets. In the subsequent sections, we show that *Aerosol Hood* operation effectively mitigates aerosol dispersal while the patient remains within the hood. While the particular design discussed is that built and tested in our laboratory, we believe the engineering bench tests and simulated hospital environments examined provide strong support for the efficacy of a number of recently developed localized negative pressure systems which are being developed in response to the COVID-19 pandemic, provided they follow similar design principles and use similar flow rates.

METHODS

Aerosol hood construction

Figure 1 displays photographs of a first-generation *Aerosol Hood* prototype as well as a 3-dimensional rendering with dimensions displayed. The hood is 27" (68.6 cm) in width and depth, enabling it to easily fit on most transport and ICU beds. The initial prototype was designed to lie on a flat bed, but can be modified with a hook system to enable use on an inclined bed as well. The patient (caudal, foot-end) opening is 25.625" (65 cm) in width and 14" (35.56 cm) in height. Two 7" (17.78 cm) diameter 2-layer iris ports (silicone rubber) on the HCW face (cranial, head-end) enable HCWs to access all areas within the hood. Similarly, iris ports on the sides allow additional HCW patient access, by placing one hand in the iris port, and the second hand through the caudal opening. The frame of the *Aerosol Hood* is ¼" (0.635 cm) thick polycarbonate. The top of the prototype is a 24" × 24" (61 cm × 61 cm) HEPA filter unit which transitions into a circular duct (2 × 2 Ultrastar Ducted HEPA Module, Midwest Production Supply, Burnsville MN). Using aluminum coated flexible hosing the outlet duct is connected to an 8-speed setting blower (AC Infinity CLOUDLINE S8), capable of providing nominally 22,840 L min^{-1} of suction without the HEPA filter (maximum noise level, 39 dBA). Using duct traverse measurements in a straight tube (of length 7 duct diameters) placed between the HEPA filter and blower, we estimate that the maximum suction flow rate in the hood is ~10,380 L min^{-1}. This yields a mean velocity at the caudal opening in excess of 72 cm s^{-1} in the absence of a patient, and above 100 cm s^{-1} (above 2.3 miles per hour) with a patient present. In testing, volunteers lying within the hood noted they could feel flow over their upper chest, but did not report any discomfort because of this flow. The nominal weight of the initial prototype was 39 lbs (17.8 kg). We remark that ongoing efforts are underway to reduce weight and device footprint, while maintaining similar or better levels of provider access, repeatability in performance, and particle collection. At the same time, handles on the top of the device enable 2 HCWs to move the device into position; to date we have found little difficulty in *Aerosol Hood* placement and removal from transport and ICU beds.

Aerosol hood performance

We examined the efficacy of the *Aerosol Hood* in reducing aerosol leakage into the environment with smoke tests, submicrometer droplet nebulizer tests, tests with volunteers lying prone in the hood, and high-fidelity mannequin simulations. First, contamination of aerosol particles outside of the hood was qualitatively characterized via smoke visualization, where a smoke candle (Superior Signal Company LLC) was ignited within the aerosol hood, both with the negative pressure blower off and blower on. Second, as depicted in Figure S1, quantitative characterization was carried out by nebulizing pure oleic acid via a Laskin nozzle aerosol generator (ATI model 4B, Owings Mills, MD) operated at ~10 L min^{-1} air flow. The resulting aerosol was sent into the hood directly via a tube positioned at the hood center. This resulted in polydisperse oleic acid droplets 50 nm to 1 micrometer in diameter with a mode size near 300 nm dispersed into the hood. The size distributions of droplets both within the hood and at 3 locations outside the hood were measured by coupling a differential mobility analyzer (DMA, custom-built, with identical dimensions to a TSI Inc. model 3081)[12] and condensation particle counter[13] (model 3025A, TSI Inc., Shoreview, MN): 15" (38.10 cm) above the aerosol outlet, 6" (15.24 cm) from (1) the rear iris ports (cranial side), (2) in the front of the hood (caudal side), and (3) the left side iris port. A Po-210 sealed source was used to ionize droplets before measurement,[14,15] and the DMA was operated with a nonrecirculating sheath

flow of filtered air at 5.7 L min^{-1}. The DMA was operated in stepping mode to determine electrical mobility distributions, from which size distributions were inverted using an in-house written Twomey-Markowski data inversion routine, similar to our group's recent efforts to characterize electrosurgical smoke particle size distributions.[16] Size distribution measurements were carried out only after 5-10 minutes of stable operation of the nebulizer and hood, and were repeated 3 times at each measurement location for each tested blower speed.

Further efficacy tests with a larger particle size range were carried out with the *Aerosol Hood* positioned on an ICU bed (Stryker Corporation, Kalamazoo, MI) within the M-Simulation center of the University of Minnesota (IRB approved STUDY00009496). Five volunteers lay supine with their head and upper torso within the hood, as depicted in Figure 1a. Simultaneously, a saline nebulizer (AirLife Misty Max 10 Disposable Nebulizer) was operated continuously at 10 L min^{-1} O_2 volumetric flow rate, generating an aerosol just inside left port (that is the volunteer's left) within the hood. Volunteers were asked to turn their head towards the nebulizer and cough twice in rapid succession, with 3 replicates. This procedure was intended to mimic aerosol dispersal through coughing, with intentional efforts to direct particles towards the iris port and hence to penetrate the hood. The nebulizer, generating submicrometer-to-supermicrometer aerosol particles, was utilized as a proxy for cough droplets; prior studies consistently revealed that the aerosol produced during coughing, speech and other mouth movements is extremely low in number concentration relative to indoor air background levels after dispersal into the environment[17-21] (measurements of such particles need to be done in clean-room facilities or closed systems) hence without the nebulizer, aerosol penetration would not be easily detectable. Size distribution measurements of particles were made

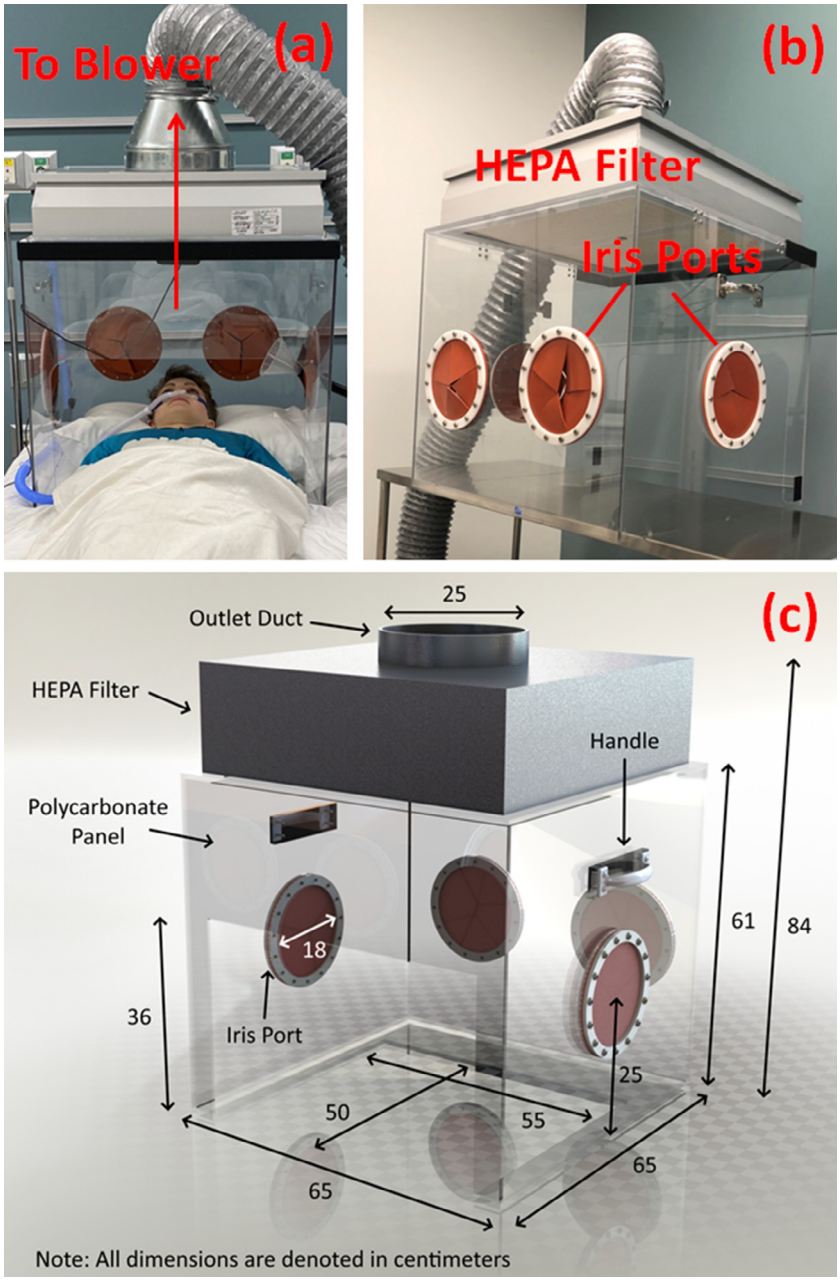

Fig 1. A photograph of a healthy volunteer (unsedated) demonstrating high flow nasal cannula within the *Aerosol Hood* (A). An angled, cranial view of the *Aerosol Hood*. (B). A 3-dimensional rendering of the *Aerosol Hood*, including dimensions in centimeters (C).

both inside the hood and outside the hood near the right iris port using a funnel inlet attached to an aerodynamic particle spectrometer (APS, TSI model 3321) measuring in a particle size range from 0.5 μm-20 μm. Fifteen successive 2 second tests were carried out in triplicate with the APS. For measurements within the hood, the funnel sampler was positioned immediately inside the left iris port (as depicted in Fig 1a), while for measurements outside, the funnel sampler was 6" (15.24 cm) from the iris port. For both DMA-CPC measurements, and APS measurements, we report the penetration as the ratio of the size distribution at an outside location, relative to the size distribution. Representative source aerosol size distributions from within the hood are shown in Figure S2 of the supporting information.

Coupled with size distribution measurements, we also aerosolized 5% by mass fluorescein (uranine) aqueous solution, which upon drying of water yielded a polydisperse fluorescein particle distribution in the 80 nm-400 nm size range. Fluorescein aerosol particles were introduced into the hood via the oral passage of a SimMan 3G patient simulator (Laerdal Medical, Stavanger, Norway) placed on a transport bed (Stryker Corporation, Kalamazoo, MI) with its head and upper torso within the hood. Aerosol dispersal was carried out for 4 minutes, while an HCW in full PPE (gloves, gown, safety glasses, and mask) inserted their arms up to the elbows inserted into the hood. By placing equal sized areas ($\sim$ 1.5 cm $\times$ 1.9 cm) of tape on 5 locations on the HCW which were within the hood (2 hands, 2 wrists, and on a CMAC handle held in the right hand) and 6 locations on the HCW outside the hood (forehead, nose, left shoulder, right shoulder, and center chest), deposited particles were sampled and quantified via desorption of the fluorescein into 3 ml 1mM NaOH aqueous solution and fluorometry using a fluorimeter (Model 450, Sequoia-Turner). As tape is often triboelectically charged, we note that particle collection onto tape may have been partially facilitated by electrostatic forces between the noncharge neutralized fluorescein particles and the tape. Therefore, while fluorescein mass concentrations between different locations can be intercompared, we do not attempt to determine true deposition rates from fluorescein measurements in the present effort.

RESULTS

Photographs taken from the rear position of the aerosol hood 30-40 seconds after ignition of a smoke candle are shown in Figure 2 both without (left) and with (right) negative pressure induced by a highspeed blower. Visually evident is the penetration of smoke through the iris ports in the absence of active flow; this demonstrates that although physical barriers can serve as impaction surfaces to collect larger expelled particles and surfaces, noninertial particles with longer lifetimes still penetrate these devices and remain aerosolized upon removal of such barriers. Conversely, active flow and filtration completely mitigate visible smoke penetration through the iris ports.

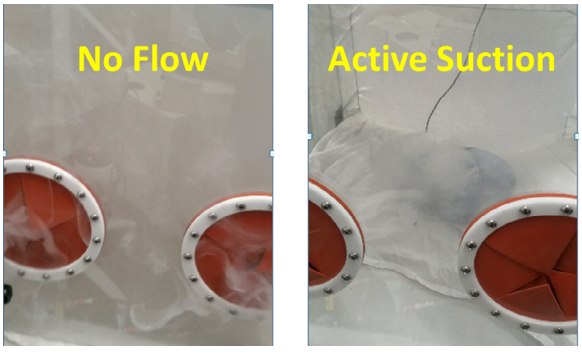

Fig 2. Photographs from the cranial side of the Aerosol Hood $\sim$ 30-40 seconds after ignition of a smoke candle within the hood. The smoke particle size distribution was not measured, but likely spans the submicrometer to supermicrometer size range. ***Left***: particles penetrate through the hood in the absence of external flow. ***Right***: With active suction at the maximum blower speed, particle penetration is not evident. A white cloth sheet was attached to the caudal side of the hood during these measurements, but only via a Velcro connection on the top, hence the caudal side was not sealed.

More quantitative characterization of the *Aerosol Hood's* ability to prevent aerosol release is possible via size distribution measurements. Size distribution measurements were carried out without negative pressure (the blower off), at an intermediate blower speed (5,190 L min^{-1}), and at the maximum blower speed (10,380 L min^{-1}). Using size distribution measurements, the aerosol hood is characterized in terms of the average particle penetration from inside to outside, defined as the ratio of the averaged size distribution at a given outside location to the size distribution measured inside the hood. The baseline size distributions inside the hood were measured for all 3 blower settings tested, as dilution via entrained flow affects size distribution measurements. Background aerosol measurements carried out in triplicate prior to all measurements and background size distributions were subtracted from all measured distributions, prior to penetration calculation. We report penetration values in Figure 3, plotting results on a logarithmic scale, and as results show little variability error bars are not included. Without blower application, penetrations are larger than 10^{-1} for all measured particles for the caudal side. This is to be expected; the caudal opening provides no means for particle collection. Nonetheless, it is important to note this as HCWs utilizing devices derived from the *Aerosol Box*[10, 22] should not expect the device to provide protection from submicrometer particles, when they are exposed to the caudal opening. For the cranial side, particle penetrations are below 10^{-1} for all particles, and below 10^{-2} for particles above 140 nm even in the absence of active suction. This does suggest that in this instance (ie, with the *Aerosol Box*), HCWs are provided a modest level of protection by the barrier. The penetration is clearly significantly reduced via application of active suction, both at half blower power and full blower power. As similar results are obtained for these conditions, we describe them in tandem. For all examined positions above 140 nm, penetrations are below 10^{-3} (ie, the particle concentration is only 0.1% of the source concentration) and above 200 nm at full blower speed particle penetrations approach 10^{-4}. We believe the increased penetration of particles at sub- 100 nm sizes is likely due to their higher diffusion coefficients; the penetration values measured are sufficiently low such that even small increases in particle penetration appear pronounced on log-scale graphs. Overall, DMA-CPC measurements of submicrometer oleic acid droplets demonstrate the efficacy of a negative pressure system in providing HCWs protection from submicrometer particles. Penetration values near 10^{-4} approach those of HEPA filter themselves (though for HEPA filters these are validated in closed systems without concentration reduction by dilution and dispersal occurring in the present study). We do remark that generated aerosol was not charge neutralized during the dispersion experiments, hence penetration values are determined for oleic acid droplets with a charged fraction likely elevated over the commonly utilized steady-state bipolar charge distribution in closed system experiments. Nonetheless, we do not anticipate electrostatic influences to strongly affect particle migration and deposition in a high-flow, *Aerosol Hood* system.

In Figure 4 we plot the penetrations resulting from saline nebulizer experiments with volunteers within the hood. Background measurements were taken before and after each volunteer, and background results were subtracted from measurements prior to penetration calculations. Results are averaged over all volunteers, but distinguished between when volunteers were coughing, and breathing. In the larger particle size range examined, particle penetrations are below 0.01, indicating that few particles can penetrate the hood.

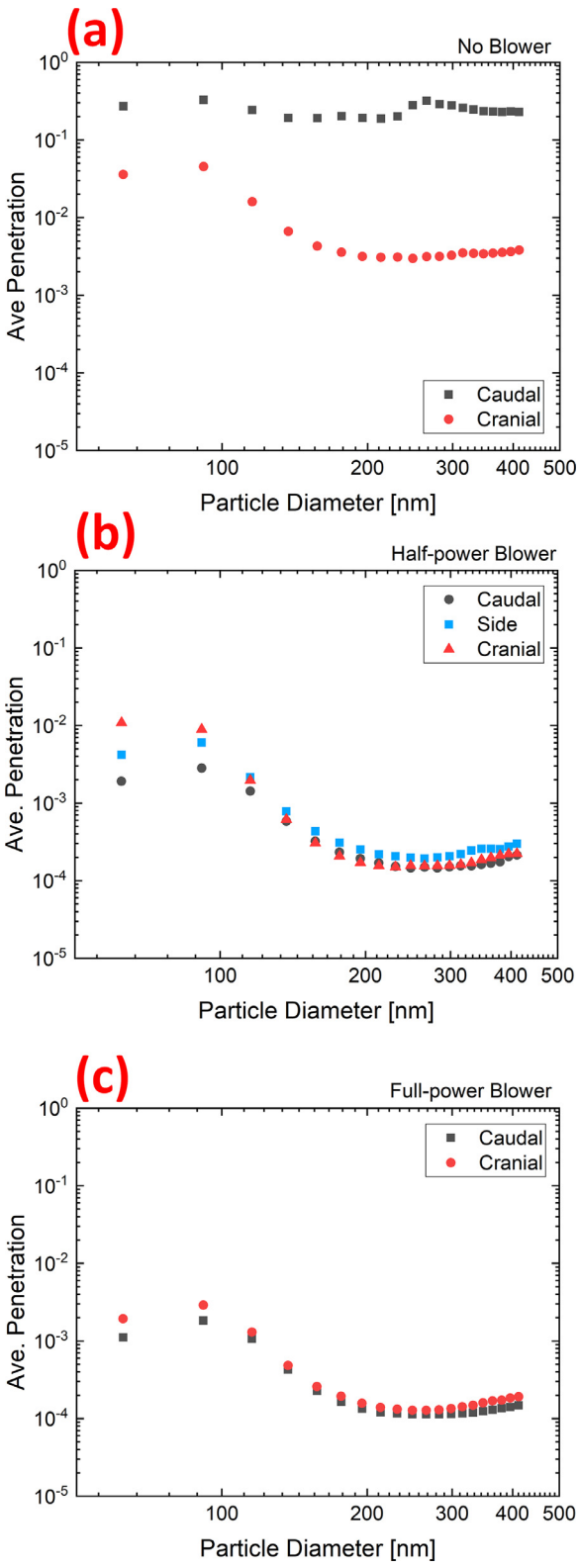

Fig 3. Average particle penetrations from DMA-CPC measurements of oleic acid particles measured at the caudal opening, cranial face, and left side of the *Aerosol Hood* without utilizing the blower (A), utilizing the blower at half power (5,190 L min^{-1}) (B), and utilizing full blower power (10,380 L min^{-1}) (C).

Presumably, the iris ports themselves can serve as impaction surfaces for larger particle deposition. Because of background subtraction, penetration calculations result in negative values for the mean

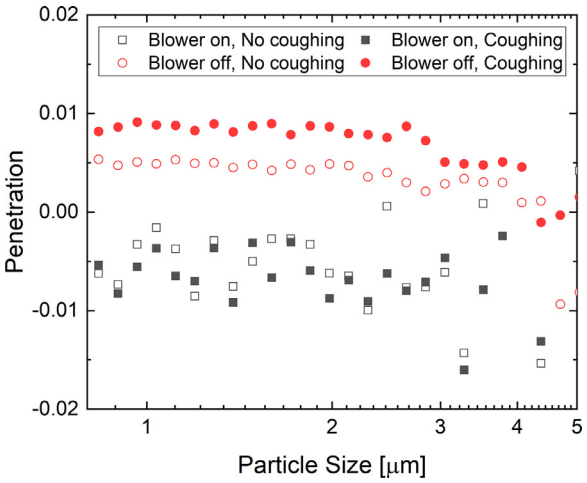

Fig 4. Background subtracted mean penetration for the left iris port, as measured via aerodynamic particle spectrometry with aerosol from a saline nebulizer operating near the left iris port. Reported values are based on size distributions averaged over all 5 volunteers and all replicates. Negative penetration values are indicative of size distribution measurements outside the hood with the blower on (maximum power), which are lower than background size distribution values.

penetration. While this is partly attributable to the finite number of volunteers, we suspect it is also because the application of the blower creates a region of depleted particle concentration near the right iris port, and the penetration microparticles from outside to inside is extremely low. Figure S3 of the supporting information show penetration plots for individual volunteers; data are noticeably more scattered without averaging over all volunteers, but penetration values never exceed 0.02 for any volunteer or any examined size, even in the absence of active suction.

Fluorescein measurements were similarly carried out in the absence of active suction, at an intermediate blower speed, the maximum blower speed, and additionally, without the hood present. In Figure 5, we combine results to report the average fluorescein concentrations (after dissolution, hence representative of relative deposition) for targeted areas inside and outside the hood. Results show clearly that application of the blower significantly reduces aerosol deposition onto PPE and surfaces outside the hood, as well as inside

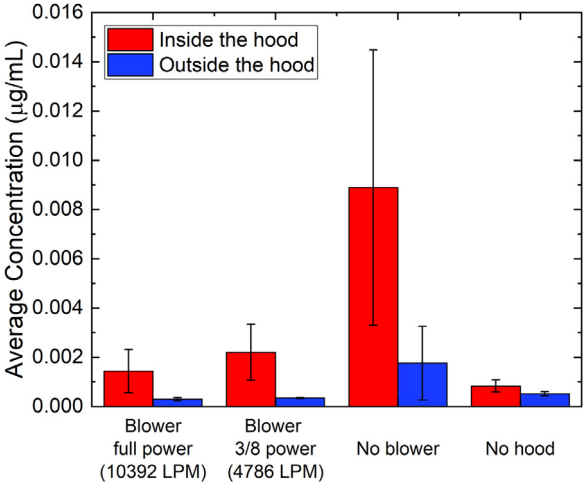

Fig 5. Average concentration of fluorescein for samples taken from inside the hood, and outside the hood using strips of tape with fluorescein later dissolved in 3 mL of 1 mM NaOH aqueous solution. Error bars denote the standard deviations of measurements.

the hood. The latter is due to a reduced aerosol lifetime in the presence of active flow, that is,. particles are driven to deposit on the filter, and not elsewhere. We also note that while the results reveal less fluorescein deposition on PPE on the hands and wrists in the absence of hood, the reduced deposition on PPE is due to the fact that in this instance, the particles generated remain aerosolized longer after the 4-minute test period and disperse throughout the room. Therefore, this result is not indicative of reduced potential for transmission, but longer range transport and longer lifetimes for aerosol particles.

DISCUSSION & CONCLUSIONS

Overall, we find that negative pressure hoods enabling HCW access to patients can be designed and implemented which have extremely low particle penetrations across a wide size range. We believe this has several promising consequences. First, aerosol hoods may enable treatments which may otherwise place HCWs at increased risk. Respiratory failure is a major concern in patients with COVID-19 infection as it can rapidly progress to acute respiratory distress syndrome. As noted in the introduction section, noninvasive positive pressure ventilation plays an important supportive role for patients with respiratory failure before more invasive therapies like mechanical ventilation are considered. However, there is the possibility of increased risk of aerosol-based disease transmission during such procedures. Loh et al[7] showed that HFNC led to increased distances traveled by respiratory secretions expelled by coughing. Leung et al[4] detected respiratory viruses such as influenza, rhinovirus, and coronavirus in exhaled breath from patient generated respiratory droplets and from aerosol particles. Based on the results obtained in our characterization trials, we propose that enclosing patients in negative pressure systems with HEPA filtration would address concerns over implementation of noninvasive positive pressure ventilation for patients with infectious respiratory diseases, providing additional protection for HCWs. During the COVID-19 pandemic, this may offload ventilator and ICU demand.

Second, during a global pandemic it is not uncommon for institutions to be operating at or beyond surge capacity. In instances like COVID-19 where the causative organism is a respiratory virus, expansion of hospital isolation capacity is crucial. Following the 2009 H1N1 influenza outbreak, hospitals were encouraged to reconsider their intensive care infrastructure expansion plans in response to gradual threats, such as the influenza pandemic. General recommendations in 2009 called on institutions to be prepared to increase their ICU capacity by 300% during a pandemic disaster.[23] Examples of isolation capacity expansion may include first utilizing all available ICU isolation space appropriately, then cohorting patients to predetermined wings or wards isolated from other noninfected patients, and finally the creation of new isolation spaces. *Aerosol Hoods* and similar devices may fill the role of “new isolation spaces,” without the need for direct modification of room configuration or building HVAC systems.

Third, it is important to note that active HEPA filtration in a rigid flow geometry system is vastly more efficient and repeatable in collecting particles than are N95 respirators. HEPA filters, at their most penetrating size, allow transmission of 3 out of 10,000 particles, while N95 respirators meet the criterion of 1 out of 20 particles transmitted at their most penetrating size and have performed poorer than this in test trials with submicrometer virus-laden particles.[24] N95 respirator filtration efficiencies can often vastly exceed the N95 “1 of 20” requirement with ideal “fit.” However, the need to fit each HCW properly is not trivial, and breathing through an N95 respirator is typically uncomfortable for wearers after sufficient durations of time.[25] Optimized *Aerosol Hoods* may protect multiple HCWs with equal to or higher collection efficiencies than achievable with passive respirators. Not only is this useful in an effort to conserve disposable PPE, but also as an engineering control, optimized *Aerosol Hoods* and related devices may reduce infection risks associated with doffing PPE,[26] as they limit deposition on PPE. We note that in most settings, engineering controls are preferred to PPE; PPE is traditionally regarded as the least effective method of exposure mitigation.

Within the University of Minnesota/Fairview health system aerosol boxes with iris ports and dimensions nearly identical to the aerosol hood presented here but without negative pressure are being actively used in patient care. Procedures performed with the aerosol boxes have included oral and nasal endotracheal intubation, Laryngeal Mask Airway (LMA) insertions, extubation, Monitored Anesthesia Care/Conscious sedation and endoscopies. HCWs have also been trained with the presented *Aerosol Hood* model and developed a disinfection protocol to apply postuse. With this protocol, the *Aerosol Hood* has been applied during terminal extubation procedures. Increased opportunities for HCWs to train with such devices, along with improved *Aerosol Hood* designs for HCW worker usability, including reduced weight and footprint may lead to routine hood application in a wider variety of procedures (eg, dental surgeries) to mitigate potential spread of infectious respiratory diseases to HCWs. We also propose that hoods may simply enable patients with COVID-19 or other infectious respiratory diseases to have greater interaction with family and friends during hospital stays. Along these lines, a potential generation 2-*Aerosol Hood* design is shown in Figure 6; in this second generation the HEPA filter is moved to side and is detachable (for cleaning or disposal, and to reduce the weight of the unit), and the cranial and top panes are adjusted to maximize visibility. In principle, hoods can be designed specifically for cord management and HCW access for specific procedures, such that the position of the hood minimally perturbs the procedure itself, the hood maintains a high level of protection against aerosol and droplet transmission, and, in the event of an emergency, the hood is easily removed without perturbing cord placement. Such design optimization has already been carried out for Neonatal Intensive Care Units (though in this instance to create a positive pressure environment), and we propose that for other purposes *Aerosol Hood* optimization can be similarly carried out, that is, with reversal of the flow Aerosol Hoods can be readily implemented for treatment of highly susceptible patients who are immunocompromised by continuously provided them with particle-free air, without the need for a positive pressure room. Finally, further refinement of such devices, including battery powered operation, may enable application for emergency medical technicians and paramedics when transporting individuals to hospitals[27] and providing care at emergency sites.

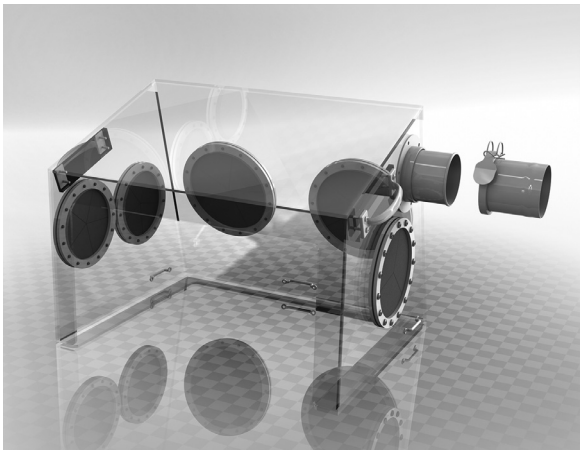

Fig 6. 3D rendering of a second generation Aerosol Hood design, with detachable HEPA filter (filter not shown, only quick-connect type fitting to the filter and blower on the right side is depicted).

Acknowledgments

The prototype Aerosol Hood was constructed by Ron Bystrom, Peter Ness, Bob Jones, and Nathan Walkington of the University of Minnesota College of Science and Engineering Machine Shop.

SUPPLEMENTARY MATERIALS

Supplementary material associated with this article can be found in the online version at https://doi.org/10.1016/j.ajic.2020.06.203.

References

1. Yang Y, Peng F, Wang R, et al. The deadly coronaviruses: The 2003 SARS pandemic and the 2020 novel coronavirus epidemic in China. *J Autoimmun*. 2020;109: 102434.
2. Uyeki T. COVID-19 Overview for Clinicians. Clinical Management of Critically Ill Adults with Coronavirus Disease 2019 (COVID-19) Webinar. 2020. Available at: https://emergency.cdc.gov/coca/calls/2020/callinfo_040220.asp. Accessed July 23, 2020.
3. NIH COVID-19 Treatment Guidelines. Oxygenation and Ventilation. Available at: https://www.covid19treatmentguidelines.nih.gov/critical-care/oxygenation-and-ventilation/. Accessed September 8, 2020.
4. Leung NHL, Chu DKW, Shiu EYC, et al. Respiratory virus shedding in exhaled breath and efficacy of face masks. *Nat Med*. 2020;26:676–680.
5. Liu Y, Ning Z, Chen Y, et al. Aerodynamic analysis of SARS-CoV-2 in two Wuhan hospitals. *Nature*. 2020;582:557–560.
6. Chia PY, Coleman KK, Tan YK, et al. Detection of air and surface contamination by severe acute respiratory syndrome coronavirus 2 (SARS-CoV-2) in hospital rooms of infected patients. *medRxiv*. 2020;11:2800.
7. Loh N-HW, Tan Y, Taculod J, et al. The impact of high-flow nasal cannula (HFNC) on coughing distance: implications on its use during the novel coronavirus disease outbreak. *Can J Anesth/Journal canadien d'anesthésie*. 2020;67:893–894.
8. Hui D, Chan M, Chow B. Aerosol dispersion during various respiratory therapies: a risk assessment model of nosocomial infection to health care workers. *Hong Kong Med J*. 2014;20(suppl 4):9–13.
9. Subhash SS, Baracco G, Miller SL, Eagan A, Radonovich LJ. Estimation of needed isolation capacity for an Airborne Influenza Pandemic. *Health Secur*. 2016;14:258–263.
10. Lai HY. Aerosol box protects healthcare providers during endotracheal intubation. 2020.
11. Thatiparti DS, Ghia U, Mead KR. An Efficient Ventilation Configuration for Preventing Bioaerosol Exposures to Health Care Workers in Airborne Infection Isolation Rooms. *AHSRAE Annual Conference*. 2017. LB-17-C005.
12. Knutson EO, Whitby KT. Aerosol classification by electric mobility: apparatus, theory, and applications. *J Aerosol Sci*. 1975;6:443–451.
13. Stolzenburg MR, Mcmurry PH. An ultrafine aerosol condensation nucleus counter. *Aerosol Sci Technol*. 1991;14:48–65.
14. Liu BYH, Pui DYH. Equilibrium bipolar charge distribution of aerosols. *J Colloid Interf Sci*. 1974;49:305–312.
15. Gopalakrishnan R, McMurry PH, Hogan CJ. The bipolar diffusion charging of nanoparticles: a review and development of approaches for non-spherical particles. *Aerosol Sci Technol*. 2015;49:1181–1194.
16. Qiao Y, Andrews AJ, Christen CE, et al. Morphological characterization of particles emitted from monopolar electrosurgical pencils. *J Aerosol Sci*. 2020;142: 105512.
17. Lindsley WG, Pearce TA, Hudnall JB, et al. Quantity and size distribution of cough-generated aerosol particles produced by influenza patients during and after illness. *J Occup Environ Hyg*. 2012;9:443–449.
18. Asadi S, Wexler AS, Cappa CD, Barreda S, Bouvier NM, Ristenpart WD. Aerosol emission and superemission during human speech increase with voice loudness. *Sci Rep*. 2019;9:2348.
19. Asadi S, Wexler AS, Cappa CD, Barreda S, Bouvier NM, Ristenpart WD. Effect of voicing and articulation manner on aerosol particle emission during human speech. *PLOS One*. 2020;15: e0227699.
20. Yang S, Lee GWM, Chen C-M, Wu C-C, Yu K-P. The size and concentration of droplets generated by coughing in human subjects. *J Aerosol Med*. 2007;20:484–494.
21. Morawska L, Johnson GR, Ristovski ZD, et al. Size distribution and sites of origin of droplets expelled from the human respiratory tract during expiratory activities. *J Aerosol Sci*. 2009;40:256–269.
22. Canelli R, Connor CW, Gonzalez M, Nozari A, Ortega R. Barrier enclosure during endotracheal intubation. *N Engl J Med*. 2020;382:1957–1958.
23. Hick JL, Christian MD, Sprung CL. Chapter 2. Surge capacity and infrastructure considerations for mass critical care. *Intens Care Med*. 2010;36:11–20.
24. Bałazy A, Toivola M, Adhikari A, Sivasubramani SK, Reponen T, Grinshpun SA. Do N95 respirators provide 95% protection level against airborne viruses, and how adequate are surgical masks? *Am J Infect Control*. 2006;34:51–57.
25. Kim J-H, Roberge RJ, Powell JB, Shaffer RE, Ylitalo CM, Sebastian JM. Pressure drop of filtering facepiece respirators: How low should we go? *Int J Occup Med Environ Health*. 2015;28:71–80.
26. Chughtai AA, Chen X, Macintyre CR. Risk of self-contamination during doffing of personal protective equipment. *Am J Infect Control*. 2018;46:1329–1334.
27. Lindsley WG, Blachere FM, McClelland TL, et al. Efficacy of an ambulance ventilation system in reducing EMS worker exposure to airborne particles from a patient cough aerosol simulator. *J Occup Environ Hyg*. 2019;16:804–816.